A&A 460, 183–190 (2006)
DOI: 10.1051/0004-6361:20065370

Astronomy & Astrophysics

A closure model with plumes

II. Application to the stochastic excitation of solar *p* modes

K. Belkacem[1], R. Samadi[1], M. J. Goupil[1], F. Kupka[2], and F. Baudin[3]

[1] Observatoire de Paris, LESIA, CNRS UMR 8109, 92195 Meudon, France
e-mail: Kevin.Belkacem@obspm.fr
[2] Max-Planck-Institute for Astrophysics, Karl-Schwarzschild Str. 1, 85741 Garching, Germany
[3] Institut d'Astrophysique Spatiale, CNRS/Université Paris XI UMR 8617, 91405 Orsay Cedex, France

Received 5 April 2006 / Accepted 22 June 2006

ABSTRACT

Context. Amplitudes of stellar p modes result from a balance between excitation and damping processes taking place in the uppermost part of convective zones in solar-type stars and can therefore be used as a seismic diagnostic for the physical properties of these external layers.
Aims. Our goal is to improve the theoretical modelling of stochastic excitation of p modes by turbulent convection.
Methods. With the help of the closure model with plume (CMP) developed in a companion paper, we refine the theoretical description of the excitation by the turbulent Reynolds stress term. The CMP is generalized for two-point correlation products so as to apply it to the formalism developed by Samadi & Goupil (2001, A&A, 370, 136). The excitation source terms are then computed with this improvement, and a comparison with solar data from the GOLF instrument is performed.
Results. The present model provides a significant improvement when comparing absolute values of theoretical amplitudes with observational data. It gives rise to a frequency dependence of the power supplied to solar p modes, which agrees with GOLF observations. It is shown that the asymmetry of the turbulent convection zone (up and downflows) plays a major role in the excitation processes. Despite an increase in the Reynolds stress term contribution due to our improved description, an additional source of excitation, identified as the entropy source term, is still necessary for reproducing the observational data.
Conclusions. Theoretical excitation rates in the frequency range $\nu \in [2.5\,\mathrm{mHz}, 4\,\mathrm{mHz}]$ now are in agreement with the observational data from the GOLF instrument. However, at lower frequencies, it exhibits small discrepancies at the maximum level of a few per cent. Improvements are likely to come from a better physical description of the excitation by entropy fluctuations in the superadiabatic zone.

Key words. convection – turbulence – Sun: oscillations

1. Introduction

Amplitudes of solar-like oscillations result from a balance between excitation and damping. Excitation is attributed to turbulent motions that excite the p modes. In the uppermost part of the convection zone, entropy fluctuations and eddy motions drive oscillations. In this region, convection becomes inefficient and there is an increase of the eddy velocities and entropy fluctuations. Solar-like oscillations are mainly excited in such a region, thus a theoretical model of the excitation processes is a powerful tool in understanding the properties of the convective zones of solar-type stars. Goldreich & Keeley (1977) have proposed a model for the excitation process using the turbulent Reynolds stress and deduced an estimation of the power supplied to the p modes. The underestimation of the excitation rates by around a factor 10^3 compared to the observed solar values (Osaki 1990) led to alternative formulations (Goldreich & Kumar 1990; Goldreich et al. 1994). Another source of excitation was identified by Goldreich et al. (1994): the so-called entropy source term. Its contribution cannot be neglected, even though Stein & Nordlund (2001) have shown that excitation from the Reynolds stress remains dominant in comparison with the entropy fluctuation source term.

Samadi & Goupil (2001) propose a generalized formalism, taking the Reynolds and entropic fluctuation source terms into account. This approach allows investigation of the effects of several models of turbulence (Samadi et al. 2003b,a) by expressing the source terms as functions of the turbulent kinetic energy spectrum and the time-correlation function.

A confrontation of this model with data from the BiSON instrument (data from Chaplin et al. 1998) led to the conclusion that the theoretical predictions were in good agreement with the observations (Samadi et al. 2003a). Nevertheless, observational data from the GOLF instrument and a study of the BiSON data indicate that some discrepancies remain between the theoretical computation and observational data. In Samadi & Goupil (2001) (see also Samadi et al. 2005), one of the main assumptions is the quasi-normal approximation (QNA), which is useful for correlation functions of the turbulent Reynolds stress and the entropy fluctuation source terms (Samadi & Goupil 2001).

The uppermost part of the convection zone being a turbulent convective system composed of two flows, the probability distribution function of the fluctuations of the vertical velocity and temperature does not follow a Gaussian law (Lesieur 1997). Thus, the use of the QNA, which is exact for a normal distribution, becomes a doubtful approximation.

In a companion paper (Belkacem et al. 2006, hereafter Paper I), we propose another approach in order to build a closure model that expresses fourth-order correlation functions in terms of the second-order ones. This alternative approach consists in considering the convection zone as composed of two flows (the updrafts and downdrafts). Starting from the Gryanik & Hartmann (2002) approach, we develop a generalized two-scale mass-flux model (GTFM) that takes the physical properties of each flow into account. Then a theoretical description of the plumes developed by Rieutord & Zahn (1995) is used to construct the closure model with plumes (CMP). This model is valid for one-point correlation functions and in the quasi-adiabatic zone. However, what is needed here is a closure model for two point correlation functions. In the present paper, we then propose a simple way to obtain this closure model to use it for calculating of the excitation rates according to Samadi & Goupil (2001). Only the Reynolds stress source term is corrected, mainly because it is the dominant term (Stein & Nordlund 2001; Samadi et al. 2003a). The entropy fluctuations are considered in the same way as explained in Samadi & Goupil (2001) (i.e. using the QNA approximation).

The paper is organized as follows: the theoretical model of stochastic excitation of p modes is briefly summarized in Sect. 2. In Sect. 3, the closure model with plume (CMP) is generalized for two-point correlation products and implemented into the formalism of Samadi & Goupil (2001). In Sect. 4, the calculation of theoretical power is explained. In Sect. 5, GOLF observational data are presented together with the derivation of observable quantities. A comparison between the theoretical power and heights computed as described in Sect. 4 with the corresponding observed quantities defined in Sect. 5 is performed in Sect. 6. Section 7 is dedicated to discussions and conclusions.

2. A model for stochastic excitation of solar-like *p* modes

The theoretical model of stochastic excitation considered here is basically that of Samadi & Goupil (2001; see also Samadi et al. 2005). It takes two sources into account that drive the resonant modes of the stellar cavity. The first one is related to the Reynolds stress tensor and as such represents a mechanical source of excitation. The second one is caused by the advection of the turbulent fluctuations of entropy by the turbulent motions (the so-called "entropy source term") and thus represents a thermal source of excitation (Goldreich et al. 1994; Stein & Nordlund 2001).

The power fed into each mode, P, is given by (see e.g. Samadi et al. 2001):

$$P \equiv \frac{\mathrm{d}E}{\mathrm{d}t} = 2\eta E = \eta \langle |A|^2 \rangle I \omega_0^2, \tag{1}$$

where $\langle\rangle$ denotes the ensemble average, $\langle |A|^2 \rangle$ the mean square amplitude, η the damping rate, and E the energy that is defined as

$$E = \frac{1}{2} \langle |A|^2 \rangle I \omega_0^2 \tag{2}$$

where I is the mode inertia and ω_0 is the oscillation eigenfrequency (see Samadi & Goupil 2001, for details).

The mean square amplitude, as explained in Samadi & Goupil (2001), is

$$\left\langle |A|^2 \right\rangle = \frac{1}{8\,\eta\,(I\omega_0)^2} \left(C_{\mathrm{R}}^2 + C_{\mathrm{S}}^2 \right) \tag{3}$$

where C_{R}^2 and C_{S}^2 are the turbulent Reynolds stress and entropy contributions, respectively. Their expressions for radial modes are given by

$$C_{\mathrm{R}}^2 = \int \mathrm{d}^3 x_0 \, \rho_0^2 \, f_{\mathrm{r}} \int_{-\infty}^{+\infty} \mathrm{d}\tau \, \mathrm{e}^{-i\omega_0 \tau} \int \mathrm{d}^3 r \left\langle w_1^2 w_2^2 \right\rangle \tag{4}$$

$$C_{\mathrm{S}}^2 = \int \mathrm{d}^3 x_0 \, g_{\mathrm{r}} \int_{-\infty}^{+\infty} \mathrm{d}\tau \, \mathrm{e}^{-i\omega_0 \tau} \int \mathrm{d}^3 r \, \langle (w s_t)_1 \, (w s_t)_2 \rangle \tag{5}$$

where w is the vertical component of the velocity, s_t the turbulent entropy fluctuation and $f_{\mathrm{r}}(\xi_{\mathrm{r}}, m) \equiv \left(\frac{\partial \xi_{\mathrm{r}}}{\partial r}\right)^2$, where ξ_{r} is the radial component of the eigenfunction, and g_{r} a function that involves the first and second derivatives of ξ_{r} (see Eq. (9) of Samadi et al. 2003b). Quantities labelled with 1 and 2 denote two spatial and temporal positions, hence $\left\langle w_1^2 w_2^2 \right\rangle$ and $\langle (w s_t)_1 \, (w s_t)_2 \rangle$ correspond to two-point fourth-order correlation products. These correlation products are usually approximated by expressions involving second-order products only (closure model). In Samadi & Goupil (2001), the simplest approximation was used i.e. the quasi-normal hypothesis. We study here consequences of using a closure model closer to reality (i.e. the CMP from Paper I). Both are recalled in the next section.

3. Closure models

3.1. The quasi-normal approximation

The QNA (Lesieur 1997, Chap. VII-2) is adopted in Samadi & Goupil (2001) as a convenient means to decompose the fourth-order velocity correlations in terms of a product of second-order vertical velocity correlations, that is, one uses

$$\begin{aligned} \langle w_1^2 w_2^2 \rangle_{\mathrm{QNA}} &= 2 \langle w_1 w_2 \rangle^2 + \langle w_1^2 \rangle \langle w_2^2 \rangle \\ \langle (w s_t)_1 \, (w s_t)_2 \rangle_{\mathrm{QNA}} &= \langle w_1 w_2 \rangle \langle s_{t1} s_{t2} \rangle , \end{aligned} \tag{6}$$

where s_t is considered as a passive scalar.

This approximation (Eq. (6)) remains strictly valid for normally distributed fluctuating quantities with zero mean. As shown by Kraichnan (1957) in the context of turbulent flows and Stein (1967) in the solar context, the cumulant (the deviation from the QNA) can be large and therefore not negligible. The CMP presented in Paper I was shown to be a significant improvement on the QNA for the one-point correlation products. However, we need two-point correlation products here (see Eqs. (4) and (5)). A generalization of the CMP for two-point correlation products is therefore developed in Sect. 3.2 below.

The second-order correlation products in Eq. (6) are expressed in the Fourier domain $(\boldsymbol{k}, \omega)$ where $\boldsymbol{k}$ and ω are the wavenumber and the frequency associated with a turbulent element (see Samadi & Goupil 2001, for details).

3.2. The closure model with plumes

The closure model with plumes (see Paper I) has been established only for one-point correlation products. Here we generalize the CMP to two-point correlation products. We start in Fig. 1 by comparing the correlation product $\langle w_1^2 w_2^2 \rangle$ calculated directly from 3D numerical simulations obtained from the Stein & Nordlund code (see Sect. 4) with those calculated using Eq. (6) of the QNA with second-order correlation products taken from the 3D simulation. The question is whether the modelling of the $\boldsymbol{k}$ dependency on the two-point correlation function by the QNA can be used. For the sake of simplicity, we assume that the QNA can be used for the ω dependency.

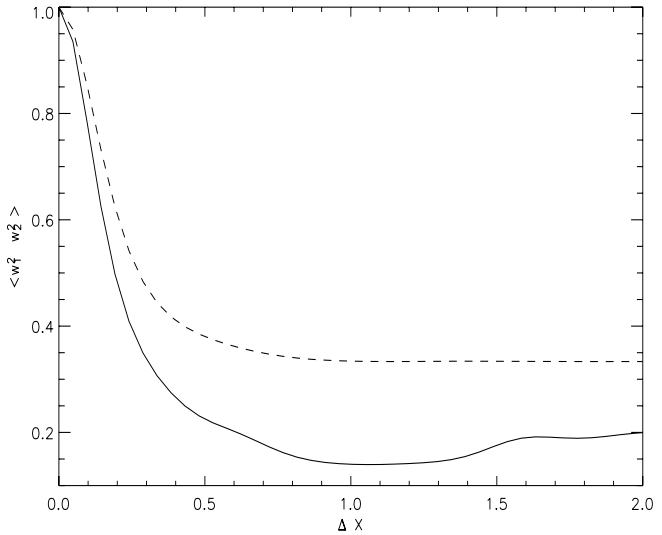

Fig. 1. Fourth-order correlation function calculated in the quasi-adiabatic zone directly from the 3D numerical simulation (solid line) and using the QNA approximation (Eq. (6); dashed lines). The fourth-order moments are presented as a function of the correlation length (ΔX), and the two curves are normalized so as to emphasise only their $\boldsymbol{k}$ dependency.

The correlation products $\langle w_1^2 w_2^2 \rangle$ in Fig. 1 are normalized so as to compare only the $\boldsymbol{k}$ dependency of these quantities. In the quasi-adiabatic region, the line width at half-maximum of the QNA and the numerical product are roughly the same. Discrepancies at high values of ΔX (the correlation length) are expected to have a negligible influence on the correlation product. Hence, we assume that the modelling of the $\boldsymbol{k}$ dependency on the two-point correlation product by the QNA is valid due to a small difference between the line width at half-maximum. Hence it is legitimate to use the $(\boldsymbol{k}, \omega)$ dependency given by the QNA. One then needs only to correct the value of the correlation product at $(\boldsymbol{k} = \boldsymbol{0}, \omega = 0)$ (which corresponds to the one point correlation function) with the CMP (see Paper I) for the turbulent Reynolds stress term contribution. We use the interpolation formula of Gryanik & Hartmann (2002) for the FOM of the velocity (Paper I, Eq. (13))

$$\langle w_1^2 w_2^2 \rangle_{\rm CMP} = \left(1 + \frac{1}{3} S_w^2\right) \langle w_1^2 w_2^2 \rangle_{\rm QNA}, \tag{7}$$

with $\langle w_1^2 w_2^2 \rangle_{\rm QNA}$ given by Eq. (6) the skewness S_w is calculated from the CMP (see Paper I for details).

In Fig. 2, calculations using Eqs. (6) and (7) are compared to the direct numerical correlation product. The above generalization of the CMP to two-point correlation products provides a good approximation mainly in the quasi-adiabatic region where the CMP is the more accurate one (see Paper I). The $\boldsymbol{k}$ dependence is approximatively modelled by the QNA (Fig. 1) except for large correlation lengths ($\Delta X > 0.2$ Mm), but these contribute only negligibly to $\langle w_1^2 w_2^2 \rangle$. However, in the superadiabatic zone, the generalization of the CMP and the QNA both fail to describe the two-point correlation function. In that zone, the temperature gradient is varying quickly, which is not the case in the CMP. In the plume model (Paper I) the temperature gradient appears only through a polytropic law, and for sake of simplicity we assume an isentropic atmosphere. In addition, for modelling the FOM $\langle w^4 \rangle$, the interpolated formula derived by Gryanik & Hartmann (2002) (Paper I, Eq. (13)) is not valid in the superadiabatic zone. Thus, in this zone the treatment of

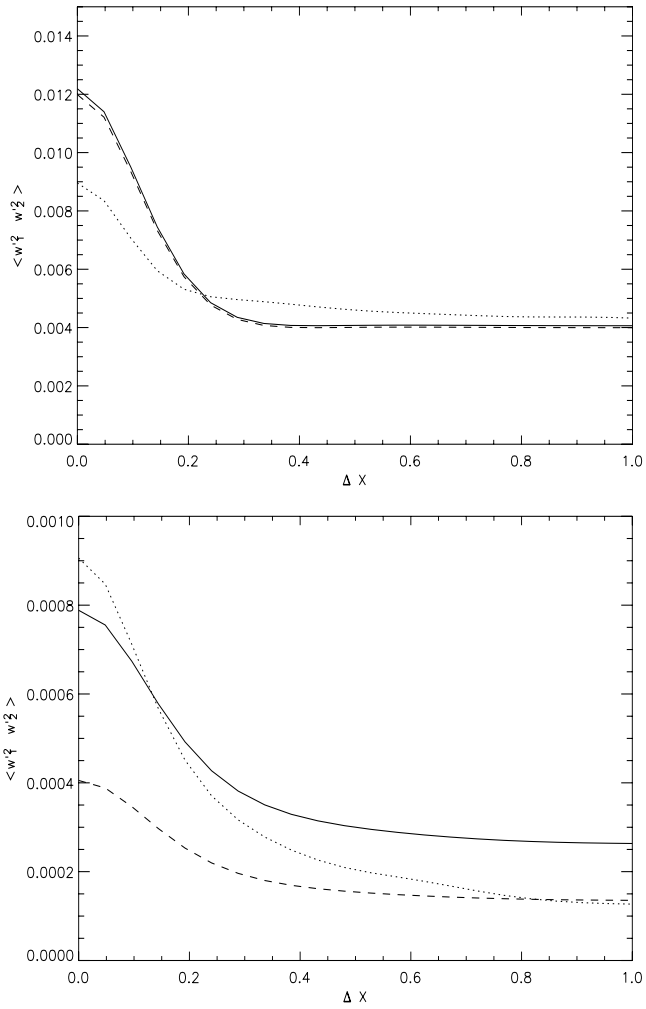

Fig. 2. Fourth-order correlation function calculated in the superadiabatic zone (at *the top*) and in the quasi-adiabatic zone (at *the bottom*) directly from the 3D numerical simulation (dotted line), using the QNA approximation (Eq. (6); dashed lines) and using the CMP (Eq. (7); solid line).

Eqs. (6) and (7) will introduce an energy excess injected into high-frequency p modes.

4. Calculation of the theoretical *p* mode excitation rates

The rate (P) at which energy is injected per unit time into a mode is calculated according to the set of Eqs. (4)−(6) when the QNA is used and Eqs. (4)−(7) using the CMP (see Sect. 4.1). The calculation thus requires the knowledge of four different types of quantities:

1) quantities that are related to the oscillation modes: the eigenfunctions ($\xi_{\rm r}$) and associated eigenfrequencies (ω_0);
2) quantities that are related to the spatial and time-averaged properties of the medium: the density ρ_0, the vertical velocity $\tilde{w}$, the entropy $\tilde{s}$, and $\alpha_{\rm s} = \partial P_0 / \partial \tilde{s}$;
3) quantities that contain information about spatial and temporal correlations of the convective fluctuations: $E(k)$, $E_{\rm s}(k)$, and $\chi_k(\omega)$;
4) quantities that take anisotropies into account: a and Φ. The value of a is the mean horizontal fractional area of the updrafts (see Paper I), whereas Φ measures the anisotropy of

turbulence and is defined according to Gough (1977; see also Samadi & Goupil 2001, for details) as:

$$\Phi = \frac{\langle w^2 \rangle}{\langle u^2 \rangle}, \tag{8}$$

where $u^2 = w^2 + u_h^2$ and u_h is the horizontal velocity.

Both a and Φ are necessary to describe the flow because a measures the geometric anisotropy between up and downflows while Φ corresponds to the measure of the velocity anisotropies. However, these two quantities are linked because of mass conservation. An explicit relation can be easily derived between them using the formalism developed in Paper I to obtain

$$\Phi = \frac{a(1-a)\delta w^2 + a\langle \tilde{w}^2 \rangle_u + (1-a)\langle \tilde{w}^2 \rangle_d}{a(1-a)\delta w^2 + a\langle \tilde{u}^2 \rangle_u + (1-a)\langle \tilde{u}^2 \rangle_d} \tag{9}$$

where the $\tilde{}$ refers to the velocities of only one flow (updraft or downdraft) and δw is defined as in Paper I. For consistency reason, a and Φ are provided by the 3D numerical simulation.

4.1. The solar case

Calculations of the eigenfrequencies and eigenfunctions (in point 1) above) are performed as in Samadi et al. (2003b) on the basis of a 1D solar model built according to Gough's (1977) nonlocal formulation of the mixing-length theory (GMLT hereafter).

The spatial and time-averaged quantities in point 2) are obtained from a 3D simulation of the solar surface. The 3D simulations used in this work were built with Stein & Nordlund's 3D numerical code (see Stein & Nordlund 1998; Samadi et al. 2003a). Two simulations with different spatial mesh grids are considered, namely $253 \times 253 \times 163$ and $125 \times 125 \times 82$, in order to verify that the results are not sensitive to the spatial mesh resolution.

Finally, for the quantities in point 3) the total kinetic energy contained in the turbulent kinetic spectrum, $E(k)$, its depth dependence, and its k-dependence are obtained directly from a 3D simulation of the uppermost part of the solar convective zone. It was found in Samadi et al. (2003a) from 3D simulations that a Gaussian – usually used for modelling χ_k – is inadequate: a Lorentzian fits the frequency dependence of χ_k best. Hence, we adopt a Lorentzian here for χ_k.

4.2. Calculation of the power injected into the solar p modes with the CMP

We use the generalized CMP for two-point correlation functions presented in Sect. 3.2 (Eq. (7)) to model the Reynolds-stress source term. By replacing Eq. (6) with Eq. (7) in Eq. (4), the calculation of $C_{\rm R}^2$ (as in Samadi & Goupil 2001) yields:

$$C_{\rm R}^2 = \frac{64}{15}\pi^3 \int_0^M {\rm d}m \,(1 + \frac{1}{3}S_w^2)\,\rho_0 \left(\frac{{\rm d}\xi_{\rm r}}{{\rm d}r}\right)^2 \int_0^\infty {\rm d}k \times \int_{-\infty}^{\infty} {\rm d}\omega \,\frac{E^2(k)}{k^4}\chi_k(\omega_0+\omega, r)\,\chi_k(\omega, r). \tag{10}$$

Equation (10) shows that the CMP causes an increase in the power injected into p modes in comparison with calculation using only the QNA. On the other hand, the entropy source term, $C_{\rm S}^2$, is still computed using the QNA closure model (see Samadi & Goupil 2001, for details).

5. Observational data and inferring observed excitation rates

The observational data set selected here for comparison with theoretical calculations was obtained with the GOLF instrument, onboard SOHO. GOLF (Gabriel et al. 1997) is a spectrometer measuring velocities of the photosphere integrated over the whole solar disc. Its location on the space platform yields a very good signal-to-noise ratio and also continuous observations (the actual duty cycle reaches almost 100%). This latter characteristic greatly improves the signal to noise ratio in the Fourier spectrum.

However, GOLF suffers from some technical problems, which restricts the measurements to one wing of the Na D_1 line instead of both wings. This results in a more difficult absolute calibration of the measured velocity and thus a possible bias (which does not exceed 20% in terms of the acoustic rate of excitation). Characteristics of the data set used here are described in Baudin et al. (2005).

These observations correspond to two periods when GOLF was observing in the same instrumental configuration (blue wing of the Na line) with a duration of 805 and 668 days, starting on April 11, 1996 and November 11, 2002, respectively. The level of solar activity was different during these two periods, but the measured excitation rate shows no dependence on activity, as the increase in width compensates for the decrease in height of the peaks, as shown by Chaplin et al. (2000) or Jiménez-Reyes et al. (2003).

The GOLF results were compared to BiSON observations and are compatible with them over a wide frequency range. A discrepancy appears at high frequency ($\nu > 3.2$ mHz). As the height and width of peaks in the Fourier spectrum are affected by the presence of noise and gaps in the data (see Chaplin et al. 2003), GOLF was chosen for the comparison model/observations. We consider only the $\ell = 1$ modes for which their properties (line-width, amplitude) are more accurately determined than the $\ell = 0$ modes (see Baudin et al. 2005, for details).

In order to compare theoretical results and observational data, the mode excitation rates are inferred from the observations according to the relation

$$P_{\rm obs}(\omega_0) = 2\,\pi\,\Gamma_\nu\,\mathcal{M}\,v_{\rm s}^2(\omega_0) \tag{11}$$

where $\mathcal{M} \equiv I/\xi_{\rm r}^2(h)$ is the mode mass, h the height above the photosphere where oscillations are measured, $\Gamma_\nu = \eta/\pi$ the mode linewidth at half maximum (in Hz), and $v_{\rm s}^2$ the mean square of the mode surface velocity. The last is derived from the observations according to

$$v_{\rm s}^2 = \pi\,H\,\Gamma_\nu\,C_{\rm obs} \tag{12}$$

where H is the maximum height of the mode profile in the power spectrum and $C_{\rm obs}$ the multiplicative constant factor that depends on the observation technique (see Baudin et al. 2005). Equation (12) supposes that the mode line profiles are symmetric, but it is well known that the mode profile deviates from a Lorentzian. However, Baudin et al. (2005) show that this equation is accurate enough for the evaluation of the mean square of the mode velocity, Eq. (12). On the other hand, the mode asymmetry is taken into account when determining mode line widths from observational data.

The mode mass is very sensitive to altitude at high frequency (see Fig. 1 of Baudin et al. 2005), so the layer (h) where the mode mass is evaluated must be properly estimated to derive correct values of the excitation rates. Indeed, solar seismic observations

in Doppler velocity are usually measured from a given spectral line. The layer where oscillations are measured then depends on the height where the line is formed. The GOLF instrument uses the Na I D 1 and D 2 lines whose height of formation is estimated at the height $h \approx 340$ km (see Baudin et al. 2005).

As an alternative to comparing theoretical results and observational data, Chaplin et al. (2005) propose to derive the maximum height of the mode profile (H) from the theoretical excitation rates and the observed mode line width according to the relation:

$$H = \frac{P}{2\pi^2 \mathcal{M} \Gamma_\nu^2 C_{\rm obs}}, \tag{13}$$

where $C_{\rm obs} = 2.59$ for $\ell = 1$ modes.

Representation of the excitation rates themselves (Eq. (11)) emphasises disagreement at high frequencies, whereas disagreement at low frequency is more apparent with a representation using the profile height (Eq. (13)). Note that in the case of the observable height, only the slopes are the meaningful quantities, as the amplitude magnitude depends on the phase of the solar cycle when the observations were recorded.

As the maximum height H strongly depends on the observation technique, one cannot compare values of H coming from two different instruments. In Fig. 6, we therefore plot the product $HC_{\rm obs}$, a quantity that is less dependent on the observational data (but still through $\mathcal{M}$). Note that for ease of notation, $HC_{\rm obs}$ is noted H in the following.

It is important to stress that the mode height (H) calculated from the theoretical excitation rates (Eq. (11)) depends on the observations through the line width Γ_ν. This is why in Figs. 5 and 6 error bars appear in the theoretical results. In any case, the observational data can be characterised by at least three main features that the theoretical calculations (see above) must reproduce:

1. the frequency dependence from low to medium frequencies ($\nu < 3$ mHz);
2. the maximum of amplitude at 3 mHz for H and the slope for frequencies between 3 and 4 mHz or a nearly flat maximum between $\nu \approx 3.8$ mHz and 4 mHz for P;
3. the slope at very high frequencies $\nu > 4$ mHz.

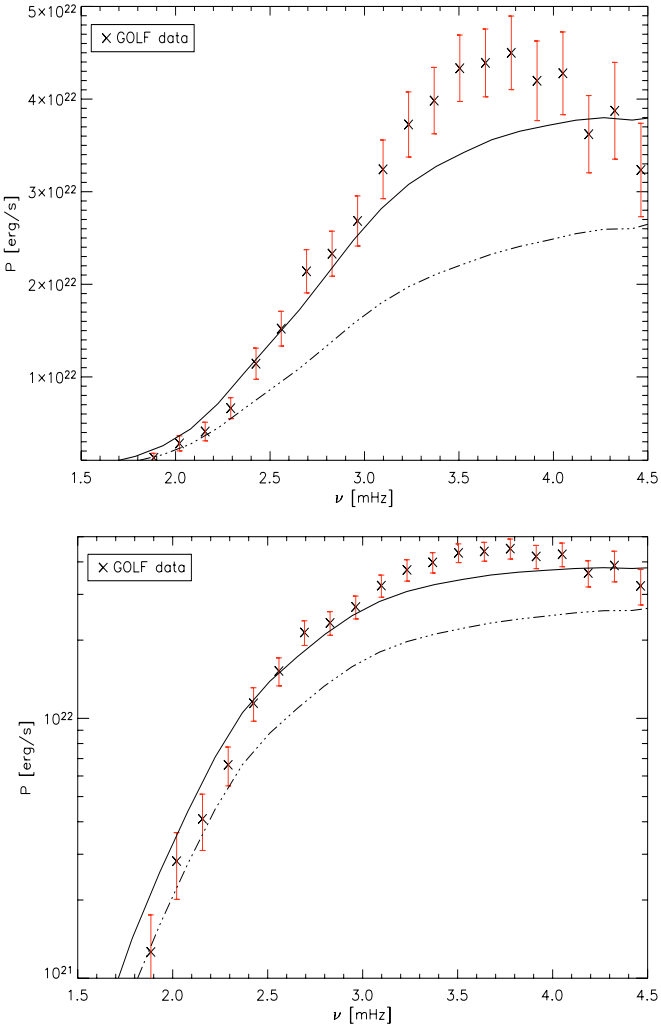

Fig. 3. Rate P at which acoustic energy is injected into the solar radial modes. *Only the Reynolds stress contribution is computed.* Cross dots represent P computed from Baudin et al. (2005) solar seismic data from the GOLF instrument (see Sect. 5). The associated error bars take into account uncertainties both from the line width (Γ_ν) and from the maximum height of the mode profile (H). The curves represent theoretical values of P computed as explained in Sect. 4: dash-dotted lines correspond to the calculation of P using the QNA closure model, and solid lines represent P using the CMP for the Reynolds stress term. We present the results in linear (at *the top*) and logarithmic scale (at *the bottom*).

6. Comparison between theoretical and observed excitation rates

6.1. Turbulent Reynolds stress contribution

Figure 3 compares the observed power P injected into solar p modes with the theoretical one computed with only the turbulent Reynolds stress term assuming either the CMP or the QNA closure models. Figure 4 shows the associated heights H as computed according to Eq. (13). The comparison shows that the closure model has a significant effect on the resulting excitation rates. Indeed, the CMP induces an increase in the energy injected into the mode by about a factor two in comparison with the QNA closure model and brings the theoretical excitation rates closer to the observational ones. This energy increase is not uniform in terms of frequencies, due to the variation in the skewness with the depth (z) (see Paper I for details) and to the fact that the mean square velocity amplitudes of the turbulent elements decrease with depth. Indeed, at the top of the convection zone where the highest frequency modes are confined, the inefficiency of the convective transport causes an increase in the velocities. Thus the effect of the flow anisotropy becomes dominant for such high-frequency modes.

At low frequencies ($\nu < 2.5$ mHz), the turbulent Reynolds stress contribution reproduces the observed power P (Fig. 3) within the observational uncertainties. As best emphasised in Fig. 4, it is possible that the theoretical results are slightly overestimated, although this remains within the observational error bars.

At intermediate frequencies ($4 > \nu > 3$ mHz), the turbulent Reynolds stress term is not sufficient to reproduce the observations, so the additional excitation coming from entropy fluctuations is necessary.

At high frequencies ($\nu > 4$ mHz), Observational data seem to indicate a decrease in the power, which is not reproduced by the theoretical power.

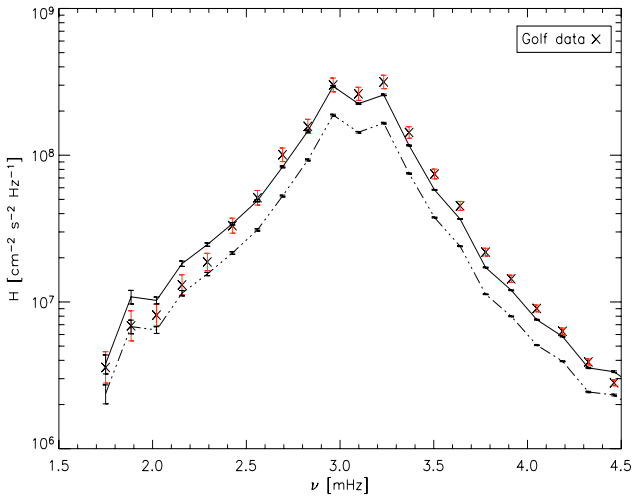

Fig. 4. Mode height H calculated as explained in Sect. 5 *using only the Reynolds stress contribution*. The solid (resp. dash-dotted) line represents H calculated with the CMP (resp. QNA) closure model, and cross-dots represent GOLF data with associated error bars. Error bars associated with the curves are due to mode line widths that are taken from observations (see Eq. (13)).

6.2. Adding the entropy fluctuation contribution

To proceed further, we add the C_S^2 contribution (Eq. (5)). Results for the excitation rate and the maximum height are presented in Fig. 5. The additional (positive) entropy contribution causes an overall increase in the excitation rates as shown in Fig. 5. The theoretical modelling now reproduces the maximum of the power supplied to the modes when compared with the observational data. For the frequency behaviour of the excitation rate and height, Fig. 5 show:

At low frequency ($\nu \in [1.6\,\mathrm{mHz}; 3\,\mathrm{mHz}]$). We pointed out in Sect. 6.1 that the contribution from the Reynolds stress term can be sufficient for reproducing the GOLF data, perhaps even overestimating it. The combination of both Reynolds stress and entropy fluctuation is too large compared with the observation, and the resulting slope differs from the observational one in this frequency domain. Note however, that in Fig. 5 error bars represent 1σ error bars (Fig. 5).

For intermediate and high frequencies ($\nu \in [3\,;4]$ mHz), the Reynolds (CMP) and entropy excitation model reproduces the ν variation in P. This is confirmed with the H representation (Fig. 5 at the bottom). However from a theoretical point of view, the description of the behaviour at high frequencies ($\nu > 4$ mHz) is more complicated because these p modes are mainly excited in the superadiabatic zone, which is difficult to model properly. On the observational side, it must be kept in mind that even data with a signal-to-noise ratio as good as GOLF lead to linewidths difficult to measure at high frequencies.

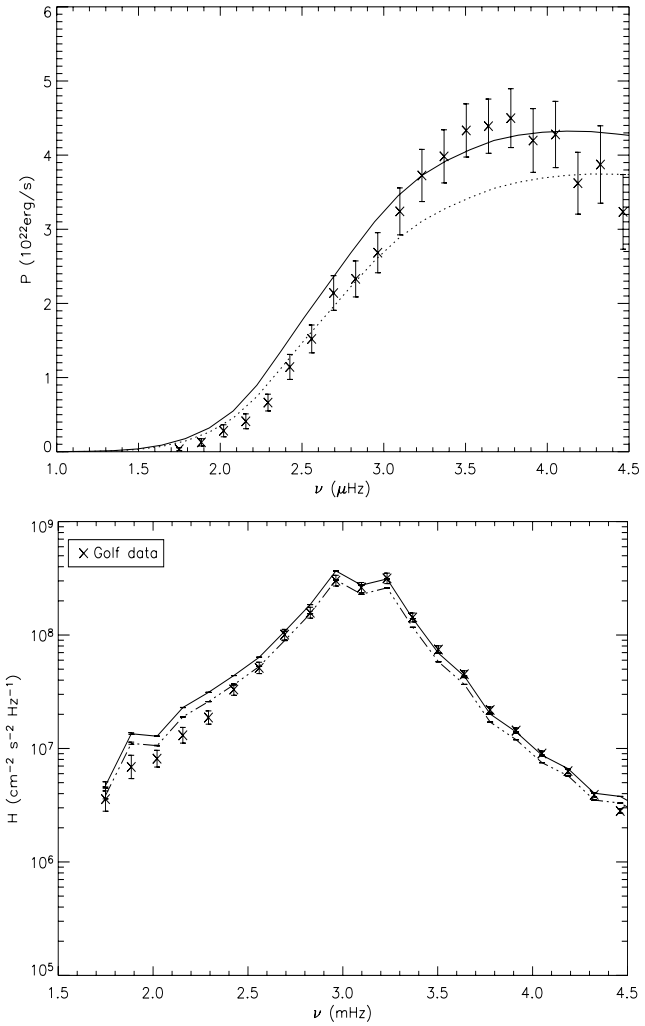

Fig. 5. *Top*: rate (P) at which acoustic energy is injected into the solar radial modes as a function of frequency. Cross dots represent P computed from the Baudin et al. (2005) solar seismic data from the GOLF instrument (see Sect. 5). The curves represent theoretical values of P computed as explained in Sect. 4: the solid line represents P using both the Reynolds stress (using the CMP) and entropy source contributions. The dotted line corresponds to the calculation for the Reynolds stress term only (using the CMP). *Bottom*: mode height (H) calculated as explained in Sect. 5. The solid line represents H calculated with the CMP closure model, *using the Reynolds stress and entropy fluctuation contributions*. The dotted line represents H computed with the CMP closure model, *using only the Reynolds stress contribution*. Cross-dots represent GOLF data with the associated error bars. Error bars associated with the curves are due to mode line widths that are taken from observations (see Eq. (13)). Only observations near minimum solar activity have been used, and they correspond to the second period as explained in Sect. 5.

7. Discussions and conclusions

We use a closure model (CMP, Paper I) that is more realistic than the usual QNA approximation to model the correlation products in a semi-analytical description of the excitation process of solar p modes. The present excitation model gives the theoretical *slope* of the power at intermediate and high frequencies ($\nu \in [2.5\,\mathrm{mHz}; 4\,\mathrm{mHz}]$), which agrees with the observed data. We also find that including the CMP causes a global increase in the injected power. This brings the power computed with the Reynolds stress contribution alone closer to (although, at intermediate frequency, still below) the observations. On the other hand, the power obtained by including both the Reynolds stress and the entropy fluctuation contributions reproduces the observations at the maximum of the excitation rates. The comparison can now be made in linear scale, hence at lower frequencies there is still a small over-estimation (which amounts roughly to a few per cents and the errors bars represent 1σ error bars). The reason for this overestimation cannot be attributed to the CMP. Indeed, the Reynolds stress contribution was compared to the

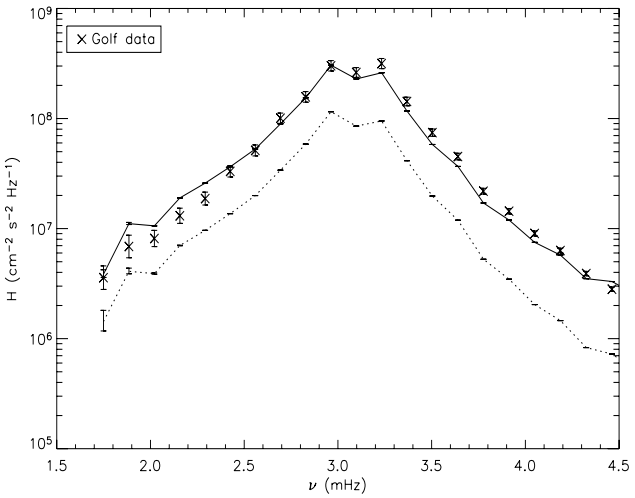

Fig. 6. Mode height H calculated as explained in Sect. 5 *using only the Reynolds stress contribution*. Solid lines represent H calculated with the CMP closure model and dots-line is the same except that a Gaussian is used for χ_k. Crosses represent GOLF data with associated error bars. Error bars associated with the curves are due to mode line widths which are taken from observation (see Eq. (13)).

3D numerical simulation (see Paper I), and the one-point fourth-order moment $\langle w^4 \rangle$ was found to agree with the simulation result. The remaining departure from the numerical simulation shows that the CMP actually underestimates the FOM in the quasi-adiabatic region, so correcting for this bias would result in an even larger overestimation of the power.

Various sources of discrepancies are likely to exist: the separation of scales used in the formalism that consists in assuming that the stratification and the oscillations have characteristic scale lengths larger than the eddies contributing to the excitation (see Samadi & Goupil 2001, for details). The physical description of the outer layers in the 1D solar model can also play an important role directly through the velocity and indirectly through the eigenfunctions. In this paper, we use Gough's (1977) non-local formulation of the mixing-lenght theory which shows an improvement in comparison with the local formulations in terms of the maximum of power P (Samadi et al. 2006) by about a few percent. Concerning the excitation model itself, some improvements in the modelling of Reynolds and entropy contributions that ought to be investigated are outlined below.

7.1. Turbulent Reynolds stress tensor contribution shortages

At low frequencies, a possibly small overestimation of the Reynolds stress contribution can be attributed to the frequency dependent factor (χ_k, see Eq. (10) in Sect. 4.1). Chaplin et al. (2005) use a Gaussian χ_k whereas Samadi et al. (2003b) use a Lorentzian factor. In Fig. 6, we present the calculation assuming a Gaussian and a Lorentzian for χ_k. As shown there, the frequency-dependent factor χ_k is likely between these two regimes. In the quasi-adiabatic convection zone, plumes are well-formed, and the convective system must be treated as composed of two flows (see Paper I). Hence, the upflows that are less turbulent can be modelled by a white noise (Gaussian), but downflows are turbulent creating a departure from a Gaussian. We expect this effect to cause a decrease in the theoretical power and bring it closer to the observation. A rough idea can be obtained by taking this effect into account as follows: we split the computation of the power supplied into the modes into two parts. Those parts correspond to upflow (χ_k: Gaussian) and to downflows (χ_k: Lorentzian). The result indicates a decrease in the power at low frequency, which brings the theoretical power closer to the observation. This is true mainly for low-frequency modes, which are less sensitive to the superadiabatic zone where plumes are formed, because this region cannot be modelled by such a simple model. This issue needs further investigation.

7.2. Entropy source contribution shortages

In the present model, the turbulent entropy fluctuations are assumed to behave as a passive scalar, in other words, the entropy fluctuations are assumed to be advected by the turbulent velocity field without dissipation. It means that the entropy field does not have any effect on the velocity field.

This assumption associated with the QNA has the advantage of simplifying the closure of the fourth-order moments involving the entropy fluctuations (see Eq. (3.1)). However the biases introduced by this assumption remain to be evaluated. If the biases turn out to be large, alternative models must be developed.

7.3. Perspectives

Finally, we stress that there is an additional dependency, the coefficient a, which is the mean fractional area of updraft on the horizontal plane (see Eq. (9)). It is a measure of the asymmetry of the flows and a small variation in its value plays a major role on the excitation rates. This parameter has been fixed here using the results of 3-D simulations. The influence of parameter a is very important, as a small variation of its value leads to an increase in power P through the skewness S_w (see Paper I). It is beyond the scope of this paper to estimate the true effect of a variation in this parameter because its value is linked to the physical properties of the flows through, for instance, conservation of the mass flux. Hence a consistent approach is to investigate a set of different numerical simulations.

The CMP closure model, indeed, strongly depends on the structure of the upper convection zone, which again emphasises that the structure of this region is very important in the theoretical prediction of the power injected into the p modes, because the skew introduced by the asymmetry increases with the departure of a from the value 0.5. It is then possible to obtain physical constraints on the asymmetry of the convection zone flows.

To understand what can affect a is therefore an important issue, and in near future it will be necessary to study the variation in a with the type of star and from a hydrodynamical point of view to determine what the main processes that are responsible for this asymmetry. One interesting issue is the influence of a magnetic field on this parameter: as described by Weiss et al. (2002) and Vögler et al. (2005), the effect of a strong magnetic field induces a reduction in the typical length scale of convection, as well as the structure of the flows (hence the value of a).

The study of the mean fractional area a as a function of the magnetic field intensity therefore represents an interesting perspective for characterising B from the excitation rates, at least for stars with an expectedly strong magnetic field.

Acknowledgements. We are indebted to J. Leibacher for his careful reading of the manuscript and his helpful remarks. We thank Å Nordlund and R. F. Stein for making their code available to us. Their code was made at the National Center for Supercomputer Applications and Michigan State University and supported by grants from NASA and NSF.

References

Baudin, F., Samadi, R., Goupil, M.-J., et al. 2005, A&A, 433, 349
Belkacem, K., Samadi, R., Goupil, M., & Kupka, F. 2006, A&A, 460, 173
Chaplin, W. J., Elsworth, Y., Isaak, G. R., et al. 1998, MNRAS, 298, L7
Chaplin, W. J., Elsworth, Y., Isaak, G. R., Miller, B. A., & New, R. 2000, MNRAS, 313, 32
Chaplin, W. J., Houdek, G., Elsworth, Y., et al. 2005, MNRAS, 360, 859
Gabriel, A. H., Charra, J., Grec, G., et al. 1997, Sol. Phys., 175, 207
Goldreich, P., & Keeley, D. A. 1977, ApJ, 212, 243
Goldreich, P., & Kumar, P. 1990, ApJ, 363, 694
Goldreich, P., Murray, N., & Kumar, P. 1994, ApJ, 424, 466
Gough, D. O. 1977, ApJ, 214, 196
Gryanik, V. M., & Hartmann, J. 2002, J. Atm. Sci., 59, 2729
Jiménez-Reyes, S. J., García, R. A., Jiménez, A., & Chaplin, W. J. 2003, ApJ, 595, 446
Kraichnan, R. H. 1957, Phys. Rev., 107, 1485
Lesieur, M. 1997, Turbulence in fluids (Kluwer Academic Publishers)
Osaki, Y. 1990, in Lecture Notes in Physics: Progress of Seismology of the Sun and Stars, ed. Y. Osaki, & H. Shibahashi (Springer-Verlag), 75
Rieutord, M., & Zahn, J.-P. 1995, A&A, 296, 127
Samadi, R., & Goupil, M. 2001, A&A, 370, 136
Samadi, R., Goupil, M., & Lebreton, Y. 2001, A&A, 370, 147
Samadi, R., Nordlund, Å., Stein, R. F., Goupil, M. J., & Roxburgh, I. 2003a, A&A, 404, 1129
Samadi, R., Nordlund, Å., Stein, R. F., Goupil, M. J., & Roxburgh, I. 2003b, A&A, 403, 303
Samadi, R., Kupka, F., Goupil, M. J., Lebreton, Y., & van't Veer-Menneret, C. 2006, A&A, 445, 233
Stein, R. F. 1967, Sol. Phys., 2, 385
Stein, R. F., & Nordlund, A. 1998, ApJ, 499, 914
Stein, R. F., & Nordlund, Å. 2001, ApJ, 546, 585
Vögler, A., Shelyag, S., Schüssler, M., et al. 2005, A&A, 429, 335
Weiss, N. O., Proctor, M. R. E., & Brownjohn, D. P. 2002, MNRAS, 337, 293